Turkish Journal of Electrical Engineering and Computer Sciences

Volume 22 | Number 6 Article 16

1-1-2014

Dynamics, stability, and actuation methods for powered compass gait walkers

KORAY KADİR ŞAFAK

TÜBİTAK

Turkish Journal of Electrical Engineering & Computer Sciences

http://journals.tubitak.gov.tr/elektrik/

Research Article

Turk J Elec Eng & Comp Sci
(2014) 22: 1611 – 1624

doi:10.3906/elk-1209-34

Dynamics, stability, and actuation methods for powered compass gait walkers

Koray Kadir ŞAFAK*
Department of Mechanical Engineering, Yeditepe University, Ataşehir, İstanbul, Turkey

Received: 07.09.2012 • **Accepted:** 05.03.2013 • **Published Online:** 07.11.2014 • **Printed:** 28.11.2014

Abstract: In this paper, methods to achieve actively powered walking on level ground using a simple 2-dimensional walking model (compass-gait walker) are explored. The walker consists of 2 massless legs connected at the hip joint, a point mass at the hip, and an infinitesimal point mass at the feet. The walker is actuated either by applying equal joint torques at the hip and ankle, by an impulse applied at the toe off, immediately before the heel strike, or by the combination of both. It is shown that actuating the walker by equal joint torques at the hip and ankle on level ground is equivalent to the dynamics of the passive walker on a downhill slope. The gait cycle for the simplified walker model is determined analytically for a given initial stance angle. Stability of the gait cycle by an analytical approximation to the Jacobian of the walking map is calculated. The results indicate that the short-period cycle always has an unstable eigenvalue, whereas stability of the long-period cycle depends on selection of the initial stance angle. The effect of the torso mass by adding a third link attached at the hip joint is investigated. The torso link is kept in the vertical position by controlling the torque applied to it. The proportional-derivative control law is utilized to regulate the angular position error of the torso link. Using linearized dynamics for this walker, active control is applied to the ankle, which reduces the dynamics of the walker to the passive walker without the torso. The proposed walker is capable of producing stable walking while keeping the torso in an upright position.

Key words: Robot dynamics, bipeds, legged robots, passive walking, stability

1. Introduction

Legged locomotion has been chosen by nature due to its particularly good adaptation in natural terrains. Achieving successful biped locomotion relies on the coordination of mechanics and control. A good understanding of biped locomotion can be obtained by exploring passive walking mechanisms. A variety of passive and semiactive mechanisms were investigated by McGeer [1,2]. These mechanisms suggest that achieving stable human-like locomotion does not necessarily require complicated motor control. For example, a planar mechanism with 2 legs connected at the hip joint can produce stable walking motion when released down a slight slope. It acts like a double pendulum with one leg (stance) in contact with the ground and the other leg (swing) free to rotate. This system exhibits a stable limit cycle, i.e. when perturbed slightly, it will return to its initial trajectory. Fully passive walkers can achieve downhill walking without any actuation and control. On the other hand, uphill walking or negotiating uneven terrain requires some control but is still relatively easy to achieve. Physical models of passive walking devices demonstrate their capability of producing stable human-like walking motion [3–5].

The simplest special case of passive dynamic walkers was presented by Garcia et al. [6]. This model

*Correspondence: safak@yeditepe.edu.tr

had 2 rigid massless legs connected by a rotational joint at the hip, a point mass at the hip, and infinitesimal point-masses at the feet. Plastic collisions occurred between the feet and the ground during heel strike instants. The interference between the feet and the ground at the mid-swing phase (foot-scuffing) is ignored. This model exhibits stable 2 period–1 gait cycles for a range of slopes. Increasing the slope yields stable higher period gaits but the walking-like motions become chaotic through period doublings. It has been reported that these walkers are capable of walking near-zero slopes [7]. These walkers exhibit 2 gait patterns at arbitrarily small slopes, and the longer step gait is stable at small slopes.

Methods for actively powered locomotion of a simplest walking model were explored by Kuo [8]. One approach was to apply a toe-off impulse immediately before the heel strike; another was to apply a hip torque between the swing and stance legs. It was found that the toe-off actuation is advantageous compared to other types of actuation because it decreases the collision loss at heel strike. Other methods for active walking on level ground were also presented [9–11]. Studies in passive dynamic walkers have revealed that energy-efficient bipedal robots that can exhibit human-like locomotion could be built without very complicated controllers [12].

A passive dynamic walking model incorporated with an upper body can be made to exhibit stable walking motion [13]. Chyou et al. [14] reported that adding a torso to the compass-gait walker improves stability and walking speed when walking downhill. Gomes and Ruina [15] demonstrated that by adding a swinging torso, the walker can be even made to walk with zero energy (no collision loss). Narukawa et al. [16] suggested an optimization-based control scheme for a planar biped walker with a torso and hip actuators. There have been studies that attempted to correlate results obtained from dynamic walking models with human gait data [17,18] and identify human gait based on image recognition techniques [19,20].

In this work, a hybrid method to produce the stable walking of a 2-dimensional (2D) walker on level ground is presented. It is shown that applying equal joint torques at the hip and ankle joints can actuate the walker. This actuation method produces a motion trajectory that is equivalent to the motion of the walker on a downhill slope with the applied torque being equal to the amount of the downhill slope. Another actuation method is to use a toe-off impulse at the heel strike, as described by Kuo [8]. The presented hybrid actuation method utilizes the application of both hip/ankle torque and a toe-off impulse. For a given toe-off impulse, a corresponding hip/ankle torque that produces a stable fixed gait can be found. For the selected actuation method and initial walker configuration, the fixed gait is determined analytically. The stability of the fixed gait is analyzed by an analytical approximation method. The effect of the added torso on the stability and performance is investigated. The actively controlled torso is stabilized in a vertical position by a proportional-derivative (PD)-type control law. The application of a computed torque control at the ankle joint reduces the dynamics of the walker on the simplified 2D walker without the torso.

2. Powered compass gait walker model

The compass-gait walker model with the additional hip and ankle torques is shown in Figure 1. The walker has 2 links with length ℓ, a point mass of M at the hip, and 2 point masses βM at the feet, where β is a positive constant. Three actuation methods are possible to achieve walking: 1) pure external torque inputs, τ_1 and $\beta\tau_2$, at the ankle and hip joints respectively; 2) a pure impulse force P at the swing foot just the before toe off; and 3) the hybrid actuation method, which is basically a combination of the torque inputs and impulse force. In the general case, the walker is on a ground slope of γ, the stance leg has an angle of θ with respect to ground normal (called stance angle), and the swing leg is at an angle ϕ with respect to the stance leg (called

swing angle). Taking the limit as $\beta \to 0$ (i.e. infinitesimal feet masses and infinitesimal torque applied between the stance and swing), the dynamics of the actively powered compass-gait 2D walker is expressed as:

$$\sin(\gamma - \theta) + \ddot{\theta} = \tau_1, \tag{1}$$

$$\sin(\gamma + \phi - \theta) - \dot{\theta}^2 \sin\phi + \ddot{\phi} + \ddot{\theta}\,(-1 + \cos\phi) = \tau_2. \tag{2}$$

Please note that the dynamic equations given throughout the paper use mass terms normalized by M, lengths normalized by ℓ, and time normalized by $\sqrt{\ell/g}$. Equations of motion (Eqs. (1) and (2)) can be linearized at about $\theta = 0$, $\phi = 0$, $\gamma = 0$, $\dot{\theta} = 0$ to yield an approximate simplified form, as follows:

$$\gamma - \theta + \ddot{\theta} = \tau_1, \tag{3}$$

$$\gamma + \phi - \theta + \ddot{\phi} = \tau_2. \tag{4}$$

The ground contact is modeled as a perfectly inelastic collision. McGeer showed that the postcollision state of the walker could be found using conservation of the momentum equations [1]. Garcia et al. [3] derived the state transition equations for the simplest walker model, and Kuo [8] modified these equations to include the effect of toe-off impulse P, applied to the stance foot, and directed at the center of mass:

$$\begin{bmatrix} \theta \\ \dot{\theta} \\ \phi \\ \dot{\phi} \end{bmatrix}^{+} = \begin{bmatrix} -1 & 0 & 0 & 0 \\ 0 & \cos(2\theta) & 0 & 0 \\ -2 & 0 & 0 & 0 \\ 0 & \cos(2\theta)\,(1 - \cos(2\theta)) & 0 & 0 \end{bmatrix} \begin{bmatrix} \theta \\ \dot{\theta} \\ \phi \\ \dot{\phi} \end{bmatrix}^{-} + \begin{bmatrix} 0 \\ \sin(2\theta) \\ 0 \\ (1 - \cos(2\theta))\sin(2\theta) \end{bmatrix} P, \tag{5}$$

where superscripts – and + indicate the conditions before and after the heel strike for that variable. The initial conditions of the walker are given by the following set of equations:

$$\begin{aligned} \theta(0) &= \theta_0 \\ \dot{\theta}(0) &= \dot{\theta}_0 \\ \phi(0) &= 2\theta_0 \\ \dot{\phi}(0) &= \dot{\theta}_0\,(1 - \cos(2\theta_0)) \end{aligned} \quad . \tag{6}$$

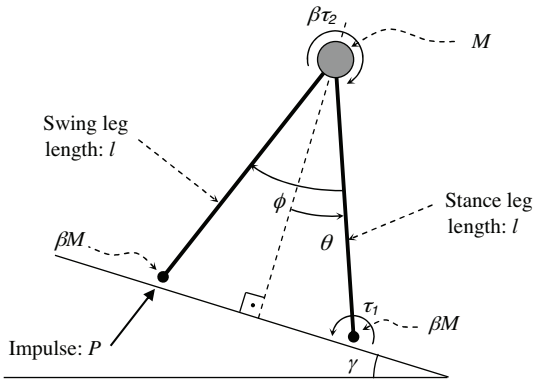

Figure 1. Compass gait walker model with hip and ankle torques.

2.1. Finding the fixed gait on level ground

Having the exact same gait pattern repeatedly at every step of the walker is referred to as a fixed gait. In order to find the fixed gait of the walker on level ground ($\gamma = 0$), simplified equations of motion for the 2D walker (Eqs. (3) and (4)) are solved analytically. Equal and constant torques, τ, at the both hip and ankle are applied. The solution to Eqs. (3) and (4) using the initial conditions in Eq. (6) gives the stance and swing angle trajectories:

$$\theta(t) = -\tau + (\theta_0 + \tau)\cosh t + \dot{\theta}_0 \sinh t, \tag{7}$$

$$\phi(t) = \frac{1}{2}\left[(3\theta_0 - \tau)\cos t + (\theta_0 + \tau)\cosh t + \dot{\theta}_0\left[1 - 2\cos(2\theta_0)\right]\sin t + \dot{\theta}_0 \sinh t\right]. \tag{8}$$

This solution includes the initial stance angle and its derivative. The existence of a fixed gait depends on the selection of the initial conditions $\left(\theta_0, \dot{\theta}_0\right)$ and a set of actuation parameters (P, τ). The period of the resulting fixed gait, T, also depends on these parameters. The applied torque and initial stance angular rate for a given set of the initial stance angle and toe-off impulse are found as:

$$\tau = \coth\left(\frac{T}{2}\right)\tan(\theta_0)\left[P - \theta_0 \coth\left(\frac{T}{2}\right)\tan(\theta_0)\right], \tag{9}$$

$$\dot{\theta}_0 = -\theta_0 \cos(2\theta_0)\coth\left(\frac{T}{2}\right)\sec^2\theta_0 - P\tan\theta_0. \tag{10}$$

When the actuation is given by a pure toe-off impulse, the hip/ankle torque will be 0 and the applied impulse will be its maximum, which is given by:

$$P_{\max} = \theta_0 \coth\left(\frac{T}{2}\right)\tan\theta_0. \tag{11}$$

At the heel strike, the angular positions and rates of the walker transition to its respective initial conditions, as defined by Eq. (5). The existence of a fixed gait requires a compatibility condition to be met: $\phi(T) = 2\theta(T)$. The fixed gait period, T, is obtained by solving this compatibility condition numerically.

Effects of the initial stance angle and applied toe-off impulse on the fixed gaits are evaluated. Short-period and long-period gaits are found (see Figure 2). The required hip/ankle torque varies with the applied impulse. The maximum amount of torque needs to be applied for a zero toe-off impulse, and maximum amount of toe-off impulse needs to be applied for zero torque. The short period increases with an increasing the impulse, whereas the long period decreases with an increase in the impulse. The short-period gait for the full impulse actuation is exactly equal to π.

3. Mimicking passive dynamic walking

The simplified equations for a passive dynamic walker going down a downhill slope θ_1 are obtained by the setting $\tau_1 = \tau_2 = 0$ in Eqs. (3) and (4) as:

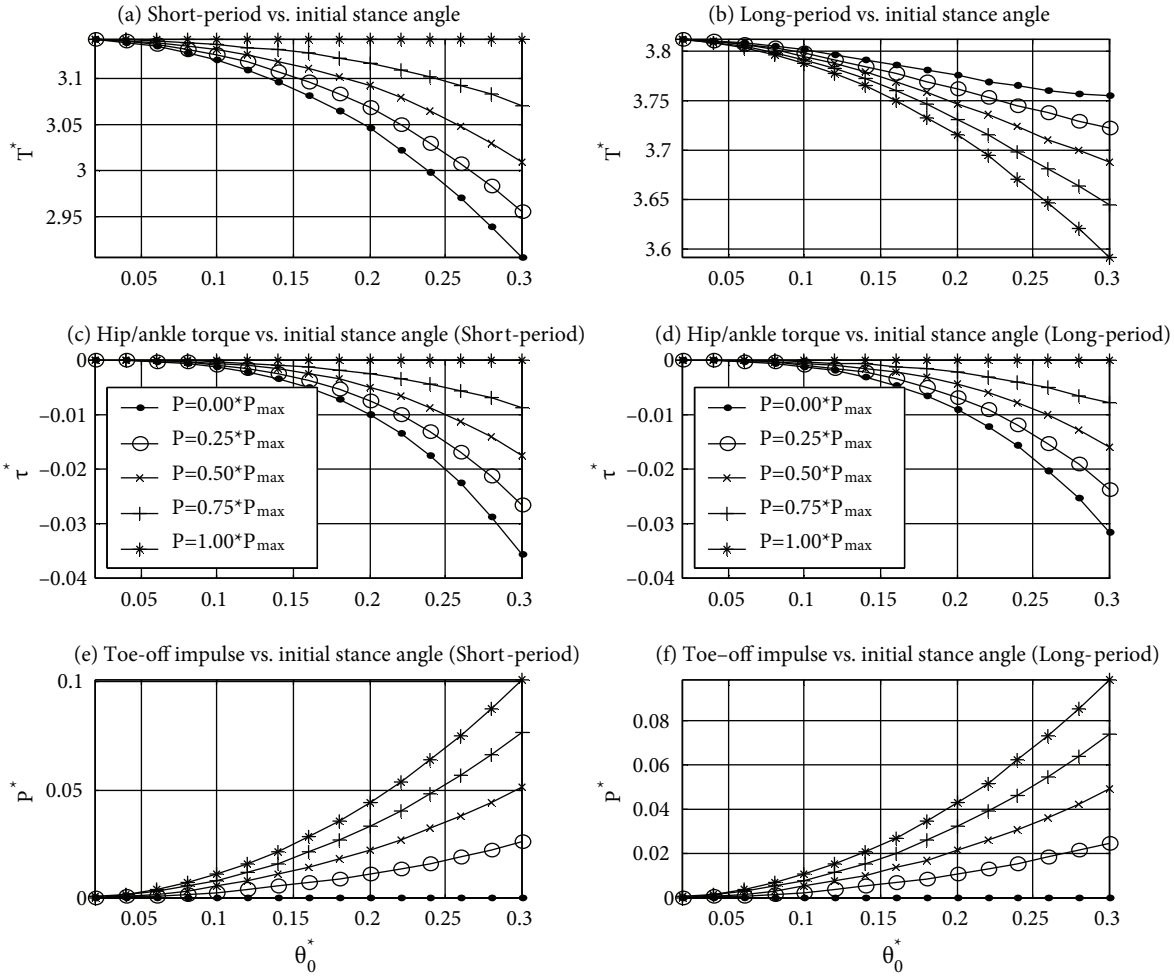

Figure 2. Short-period and long-period gaits for the 2D compass-gait walker, simplified dynamics: a) short gait period, b) long gait period, c) required hip/ankle torque for stable walking on level ground (short-period), d) hip/ankle torque for stable walking on level ground (long-period), e) required toe-off impulse for stable walking on level ground (short-period), and f) required toe-off impulse for stable walking on level ground (long-period).

$$\gamma_1 - \theta_1 + \ddot{\theta}_1 = 0, \tag{12}$$

$$\gamma_1 + \phi_1 - \theta_1 + \ddot{\phi}_1 = 0. \tag{13}$$

where θ_1 and ϕ_1 are the stance and swing trajectories. It is possible to obtain the same trajectory for a different slope with the application of a hip and ankle torque. Adding $\gamma_2 - \gamma_1$ to both sides of Eqs. (12) and (13) yields:

$$\gamma_2 - \theta_1 + \ddot{\theta}_1 = \gamma_2 - \gamma_1. \tag{14}$$

$$\gamma_2 + \phi_1 - \theta_1 + \ddot{\phi}_1 = \gamma_2 - \gamma_1. \tag{15}$$

Eqs. (14) and (15) indicate that the powered walker with an applied hip and ankle torque $\tau = \gamma_2 - \gamma_1$ on a slope γ_2 will follow the same trajectory of the passive walker on slope γ_1. Although this observation is based on the simplifying assumption that the angles are small, simulations using the dynamic equations in the original form (Eqs. (1) and (2)) validate this method to some extent. Fixed long-period-1 gaits for the fully passive

walker are computed first. It is known that the long-period-1 gait of the passive walker has stable eigenvalues [1]. The ground slope versus the fixed-gait stance angle is shown in Figure 3a. The passive dynamic walker trajectory on a level surface is obtained by applying a hip/ankle torque that is equal to $\tau = -\gamma_1$ (see Figure 3b). Simulation results based on the dynamic equations in the original form (Eqs. (1) and (2)) indicate that the active walker trajectory is almost identical to that of the passive walker. Initial stance angles resulting in a fixed gait in the actuated walker are plotted against those of the passive walker (see Figure 3c). Simulation results are obtained for stance angles of up to 0.22 rad, after which stable period-1 gaits do not exist. Within this range, the maximum deviation between the initial stance angle of the active walker to that of the passive walker is 7.9648×10^{-4} rad.

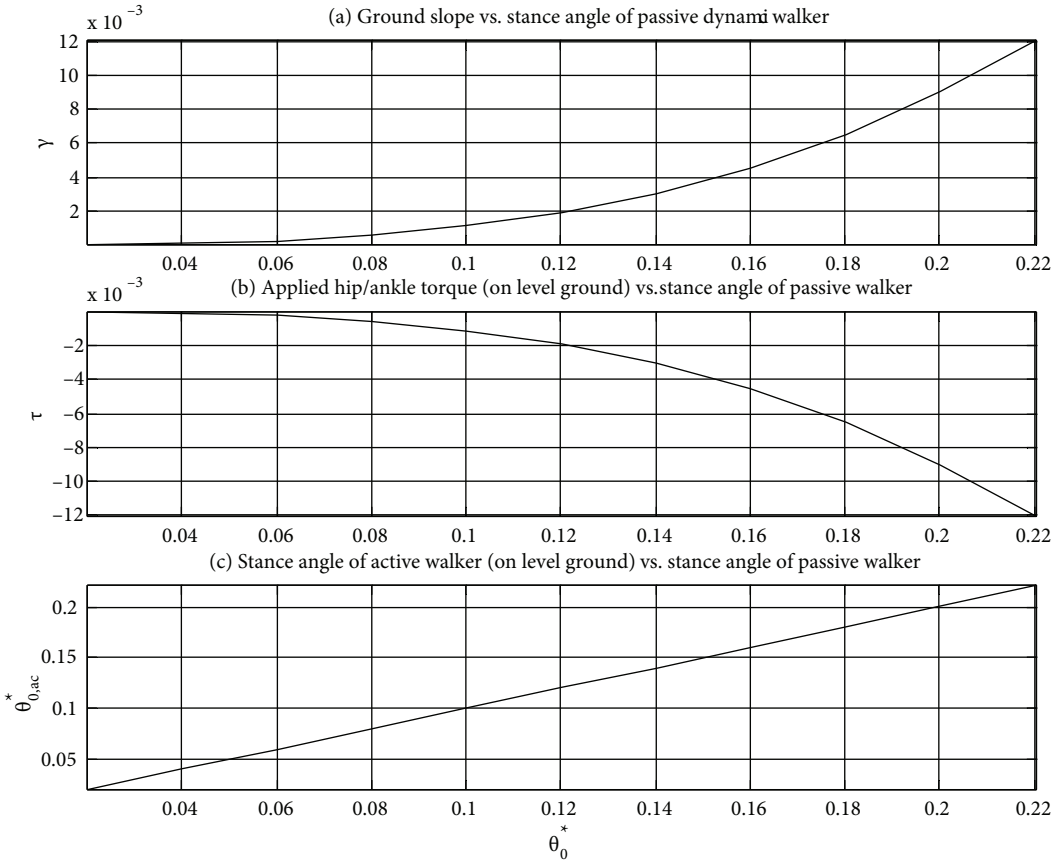

Figure 3. Hip/ankle torque actuation method: a) ground slope vs. stance angle for the fixed gait of the passive dynamic walker, b) hip/ankle torque that needs to be applied to the active walker to mimic the trajectory of the passive walker, and c) resulting fixed-gait initial stance angle for the active walker on level ground versus fixed-gait initial stance angle for the passive walker.

4. Stability of the fixed gaits

The existence of a fixed gait does not guarantee its stability. The stability of a fixed-gait cycle can be determined by the eigenvalues of the Jacobian of the stride function, $\mathbf{f}$. The stride function yields the same state of the walker after one step for a fixed-point $\mathbf{q}^*$, i.e. $\mathbf{f}(\mathbf{q}^*) = \mathbf{q}^*$. The Jacobian, $\mathbf{J}$ of the stride function has components, $\partial \mathbf{f}/\partial \mathbf{q}$, which can be computed by evaluating the stride function $\mathbf{f}$ in a small neighborhood of the fixed-point

$\mathbf{q}^*$. If all of the eigenvalues of the Jacobian are smaller than 1 in magnitude, the small perturbations to the fixed-point will decay to 0. Therefore, the system will return to its limit cycle and the fixed-gait cycle is asymptotically stable.

The Jacobian of the stride function can be numerically approximated by a method outlined by Coleman et al. [12]. In Section 2.1, the method for finding the fixed-gait of the hybrid-actuated walker is described. A fixed point, $\mathbf{q}^* = \left\{\theta_0^*, \dot{\theta}_0^*, \phi_0^*, \dot{\phi}_0^*\right\}$, along with its gait period and hip/ankle torque can be found for given initial stance angle and amount of toe-off impulse. The system is perturbed to a new state, $\mathbf{q}_0 = \left\{\theta_0, \phi_0, \dot{\theta}_0, \dot{\phi}_0\right\}$ from its fixed point as follows:

$$\begin{aligned} \theta_0 &= \theta_0^* + \Delta\theta_0 \\ \phi_0 &= \phi_0^* + \Delta\phi_0 \\ \dot{\theta}_0 &= \dot{\theta}_0^* + \Delta\dot{\theta}_0 \\ \dot{\phi}_0 &= \dot{\phi}_0^* + \Delta\dot{\phi}_0 \end{aligned} \quad . \tag{16}$$

Let us assume the system follows a new solution given by:

$$\begin{aligned} \theta(t) &= \theta^*(t) + \Delta\theta(t) \\ \phi(t) &= \phi^*(t) + \Delta\phi(t) \end{aligned} \quad . \tag{17}$$

Assuming that the simplified dynamics of the walker hold, the new solution satisfies Eqs. (3) and (4). It is shown that the perturbations satisfy the system.

$$\begin{aligned} -\Delta\theta + \Delta\ddot{\theta} &= 0 \\ \Delta\phi - \Delta\theta + \Delta\ddot{\phi} &= 0 \end{aligned} \tag{18}$$

The initial conditions for the perturbed variables must be compatible with the initial conditions of the walker states given by Eq. (6). Although there are 4 states of the walker, only 2, $\left\{\theta_0, \dot{\theta}_0\right\}$, are independent. Hence, when applying a perturbation to θ_0^*, the other variables must be selected as:

$$\begin{aligned} \Delta\dot{\theta}_0 &= 0 \\ \Delta\phi_0 &= 2\Delta\theta_0 \\ \Delta\dot{\phi}_0 &= \dot{\theta}_0^* \left[\cos(2\theta_0^*) - \cos(2\theta_0)\right] \end{aligned} \quad . \tag{19}$$

Using the initial conditions, the solution to the system of perturbation variables is found as (for perturbation to θ_0^*):

$$\begin{aligned} \Delta\theta(t) &= \Delta\theta_0 \cosh t \\ \Delta\phi(t) &= \tfrac{1}{2}\Delta\theta_0 \left(3\cos t + \cosh t\right) + \Delta\dot{\phi}_0 \sin t \end{aligned} \quad . \tag{20}$$

Similarly, when applying a perturbation to $\dot{\theta}_0^*$, the other variables must be selected as:

$$\begin{aligned} \Delta\theta_0 &= 0 \\ \Delta\phi_0 &= 0 \\ \Delta\dot{\phi}_0 &= \Delta\dot{\theta}_0 \left[1 - \cos(2\theta_0^*)\right] \end{aligned} \quad . \tag{21}$$

The solution to the system of perturbation variables for this case is as follows (for perturbation to $\dot{\theta}_0^*$):

$$\begin{aligned}\Delta\theta(t) &= \Delta\dot{\theta}_0 \sinh t \\ \Delta\phi(t) &= \tfrac{1}{2}\left(2\Delta\dot{\phi}_0 \sin t - \Delta\dot{\theta}_0 \sin t + \Delta\dot{\theta}_0 \sinh t\right)\end{aligned} \tag{22}$$

Let us expand the solutions to the perturbation variables, $\Delta\theta(t), \Delta\phi(t)$, and the fixed-gait variables, $\theta^*(t), \phi^*(t)$, around $t = T^*$, and evaluate at new gait period, T:

$$\begin{aligned}\Delta\theta(T) &= \Delta\theta(T^*) + \Delta\dot{\theta}(T^*)(T - T^*) \\ \Delta\phi(T) &= \Delta\phi(T^*) + \Delta\dot{\phi}(T^*)(T - T^*) \\ \theta^*(T) &= \theta^*(T^*) + \dot{\theta}^*(T^*)(T - T^*) \\ \phi^*(T) &= \phi^*(T^*) + \dot{\phi}^*(T^*)(T - T^*)\end{aligned} \quad . \tag{23}$$

When the heel strike condition is imposed on the perturbed system, $\phi(T) = 2\theta(T)$, one can solve for the perturbed gait period as:

$$T = T^* - \frac{[\Delta\phi(T^*) - 2\Delta\theta(T^*)]}{\left[\dot{\phi}^*(T^*) + \Delta\dot{\phi}^*(T^*)\right] - 2\left[\dot{\theta}^*(T^*) + \Delta\dot{\theta}^*(T^*)\right]}. \tag{24}$$

Hence, the state variables at gait period T are found as, $\mathbf{q}^{*-} = \left\{\theta(T), \phi(T), \dot{\theta}(T), \dot{\phi}(T)\right\}$. By applying the heel strike transition condition given in Eq. (5), one can get the state after the heel strike, $\mathbf{q}^{*+}$. For each perturbed state, one column of the Jacobian matrix is found as:

$$\mathbf{J}_i = \begin{cases} \frac{(\mathbf{q}^+ - \mathbf{q}_0)^T}{\Delta\theta_0}, & i = 1 \\ \frac{(\mathbf{q}^+ - \mathbf{q}_0)^T}{\Delta\dot{\theta}_0}, & i = 2 \end{cases} . \tag{25}$$

Stability results for the short-period and long-period gaits are obtained (see Figure 4). For the short-period gait, there is always an unstable eigenvalue. The unstable eigenvalue depends also on the selection of the applied toe-off impulse. The long-period gaits are stable for initial stance angles of up to $\sim$0.25 rad. The eigenvalues for initial stance angles less than $\sim$0.06 rad are real. Higher initial stance angles result in complex-conjugate eigenvalues; hence, absolute values for these eigenvalues are equal. Eigenvalues of the walker using the dynamic equations are presented. The difference of the eigenvalues that are computed by the analytical approximation method and by the dynamic equations is less than 0.011 in absolute value.

5. Powered compass gait walker with hip and torso mass

A third link is added to the walker model with an additional mass to simulate the effect of the torso mass. The link connected at the hip joint adds one more degree-of-freedom to the system. The walker is shown in Figure 5.

The walker is actuated by joint torques τ_1, $\beta\tau_2$, and τ_3 at the stance, swing, and torso links, respectively. The angular positions of the stance, swing, and torso links have relative angular positions of θ, ϕ, and ψ, respectively. Again the walker consists of infinitesimal point masses at the feet βM; a hip mass M; a variable torso mass αM, where α is a positive constant; and a moment of inertia I_t, which is normalized by $M\ell^2$.

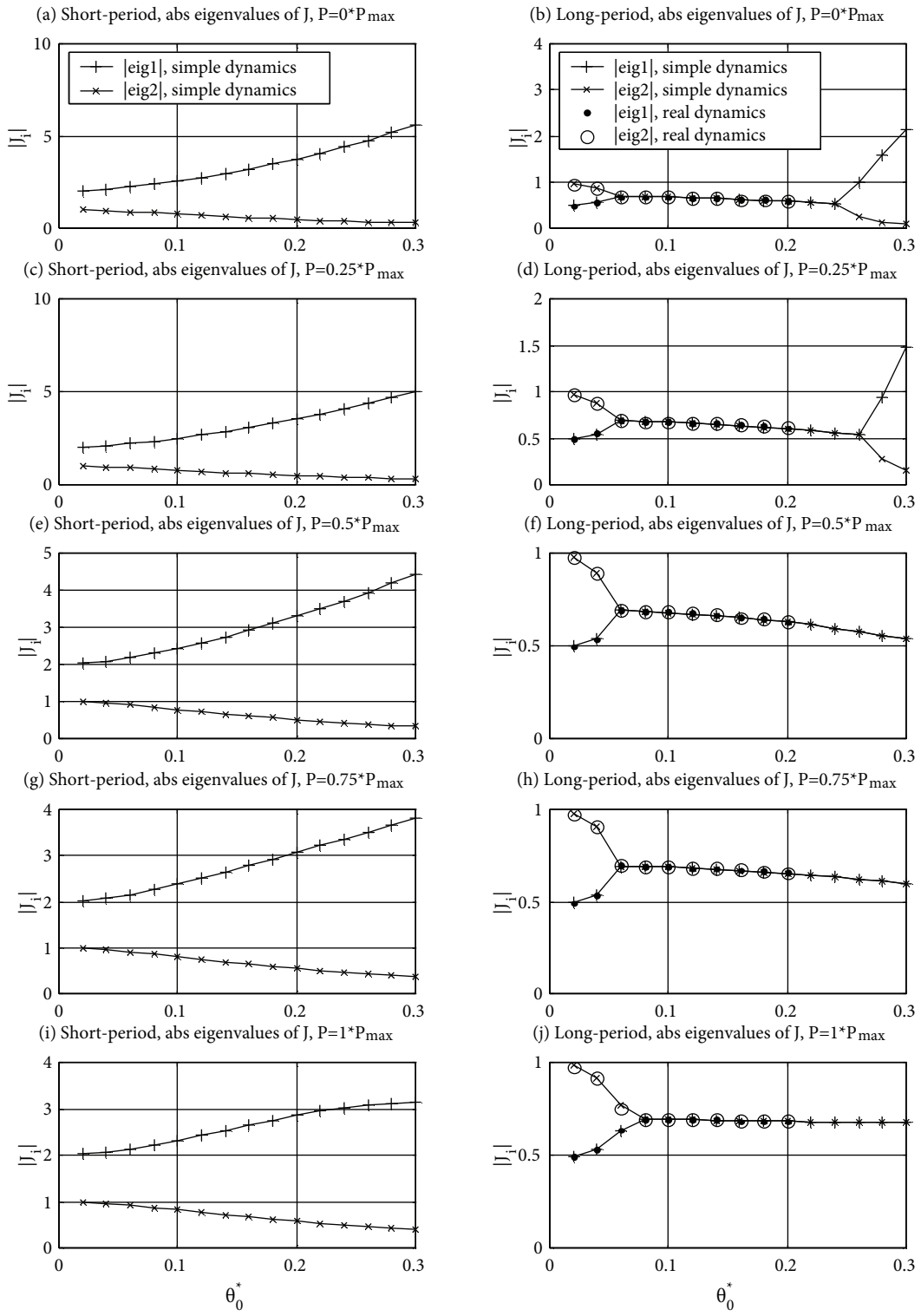

Figure 4. Absolute eigenvalues of the Jacobian for varying toe-off impulse.

The stance and swing legs both have length ℓ and the torso link has length r, which is normalized by ℓ. The dynamics of the powered walker with the hip and torso mass are found as:

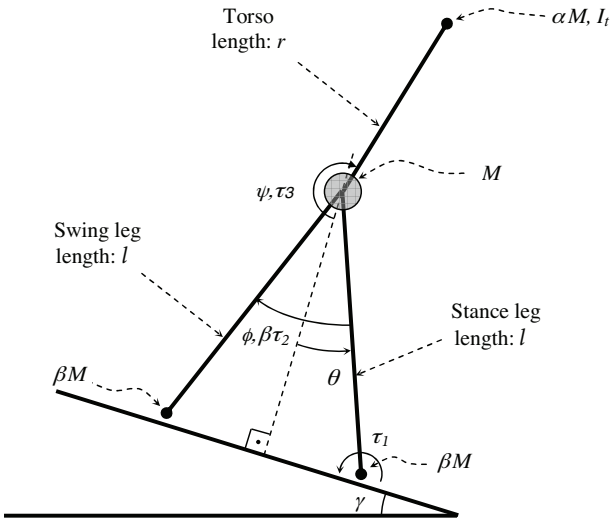

Figure 5. Powered walker with hip and torso.

$$\begin{aligned}&(1+\alpha)\sin(\gamma-\theta)+2r\alpha\left(\dot{\theta}\dot{\psi}\right)\sin\psi+\left(1+I_t+\alpha+r^2\alpha-2r\alpha\cos\psi\right)\ddot{\theta}\\&=r\alpha\sin(\gamma-\theta+\psi)+\tau_1+r\alpha\dot{\psi}^2\sin\psi+\left(I_t+r^2\alpha-r\alpha\cos\psi\right)\ddot{\psi}\end{aligned}, \tag{26}$$

$$\sin(\gamma-\theta+\phi)-\dot{\theta}^2\sin\phi+(-1+\cos\phi)\ddot{\theta}+\ddot{\phi}=\tau_2, \tag{27}$$

$$r\alpha\sin(\gamma-\theta+\psi)+\left(I_t+r^2\alpha\right)\ddot{\psi}=\tau_3+r\alpha\dot{\theta}^2\sin\psi+\left(I_t+r^2\alpha-r\alpha\cos\psi\right)\ddot{\theta}, \tag{28}$$

Knowing that the angles and their rates take small values, and the torso link is almost perpendicular, equations of motion (Eqs. (26)–(28)) can be linearized about the operating point $\theta=0$, $\phi=0$, $\psi=\pi$, $\gamma=0$, $\dot{\theta}=0$, $\dot{\psi}=0$. Thus, the following set of linear equations is obtained:

$$(1+\alpha)(\gamma-\theta)+\left[1+I_t+\alpha(1+r)^2\right]\ddot{\theta}=r\alpha(\pi-\gamma+\theta-\psi)+\tau_1+\left[I_t+\alpha r(1+r)\right]\ddot{\psi}, \tag{29}$$

$$\gamma-\theta+\phi+\ddot{\phi}=\tau_2, \tag{30}$$

$$\alpha r(\pi-\gamma+\theta-\psi)+\left(I_t+r^2\alpha\right)\ddot{\psi}=\tau_3+\left[I_t+\alpha r(1+r)\right]\ddot{\theta}. \tag{31}$$

Simultaneously solving Eqs. (29) and (31), and $\gamma-\theta+\ddot{\theta}=0$ for τ_1, and eliminating $\ddot{\theta},\ddot{\psi}$ gives:

$$\tau_1=\frac{-\left[I_t+\alpha r(1+r)\right]\tau_3+\alpha^2r^2(\pi-\psi)}{I_t+\alpha r^2}. \tag{32}$$

When the ankle torque given in Eq. (32) is applied, the system reduces down to the unpowered passive walker, given by Eqs. (3) and (4). In order to keep the torso in a vertical position, a proper joint torque, τ_3, needs to be applied. An error term is defined as the deviation of the torso from the vertical (Eq. (33)). A PD control action is utilized to minimize this error (Eq. (34)).

$$e=\psi-\theta-\pi \tag{33}$$

$$\tau_3=-ke-c\dot{e} \tag{34}$$

5.1. Heel strike transition equations

The ground contact is modeled as a perfectly inelastic collision. The angular positions of the walker just after a collision are found from geometry (stance and swing legs swapped). The angular rates are determined from the conservation of angular momentum conditions, which are:

(i) The angular momentum of the whole walker about the new contact point is conserved.

(ii) The angular momentum of the new stance leg (former swing leg) about the hip axis is conserved.

(iii) The angular momentum of the torso about the hip axis is conserved.

Hence, the angular positions of the links just after the heel strike are given by the following:

$$\begin{aligned} \theta^+ &= -\theta^- \\ \phi^+ &= -2\theta^- \\ \psi^+ &= \psi^- - 2\theta^- \end{aligned} \quad , \tag{35}$$

where the quantities with – superscripts indicate the values just before heel strike and those with + superscripts indicate the values just after the heel strike. The angular rates of the walker are given by the following:

$$\begin{aligned} \dot{\theta}^+ &= \frac{\left[2I_t(1+\alpha)+r^2\alpha(2+\alpha)\right]\cos\left(2\theta^-\right)-r^2\alpha^2\cos\left(2\theta^- -2\psi^-\right)}{2I_t(1+\alpha)+r^2\alpha(2+\alpha)-r^2\alpha^2\cos(4\theta^- -2\psi^-)}\dot{\theta}^- \\ \dot{\phi}^+ &= \frac{\left[2I_t(1+\alpha)+r^2\alpha(2+\alpha)\right]\cos\left(2\theta^-\right)-r^2\alpha^2\cos\left(2\theta^- -2\psi^-\right)}{(1+\alpha)(I_t+r^2\alpha)-r^2\alpha^2\cos^2(2\theta^- -\psi^-)}\dot{\theta}^-\sin^2\theta^- \\ \dot{\psi}^+ &= \dot{\psi}^- - 2\frac{\left[2I_t(1+\alpha)+r^2\alpha(2+\alpha)\right]\sin\theta^- + r\alpha\left[r\alpha\sin\left(3\theta^- -2\psi^-\right)-2(1+\alpha)\cos\theta^-\sin\left(2\theta^- -\psi^-\right)\right]}{2I_t(1+\alpha)+r^2\alpha(2+\alpha)-r^2\alpha^2\cos(4\theta^- -2\psi^-)}\dot{\theta}^-\sin\theta^- \end{aligned} \tag{36}$$

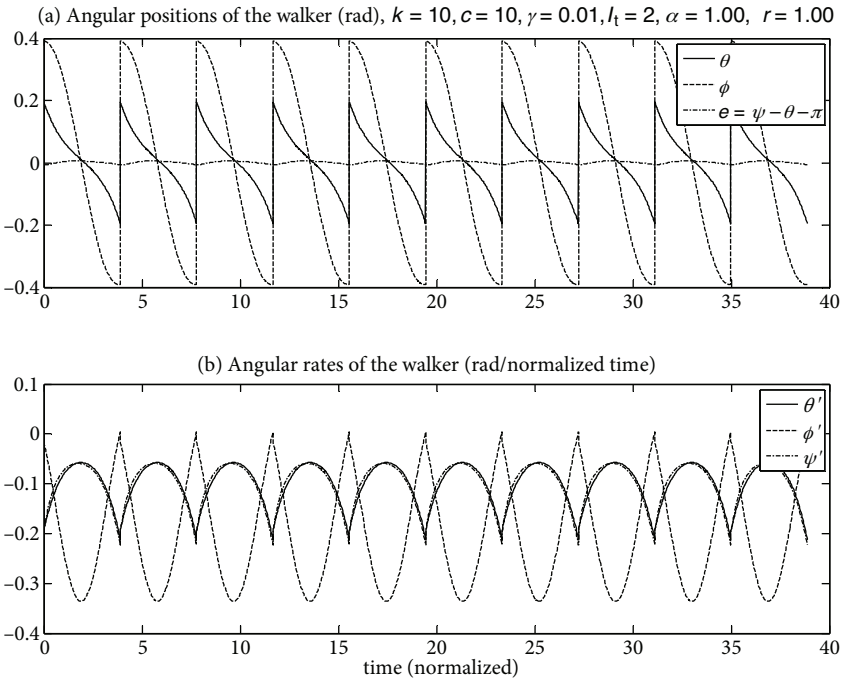

Figure 6. Stable walking pattern of the 2D powered walker with torso.

5.2. Fixed gaits and stability of the powered walker with hip and torso mass

The simulations indicate that the walker is capable of producing stable motion while keeping the torso in a vertical position (see Figure 6). The proposed control action (Eqs. (33) and (34)) is capable of keeping the error within a small deviation interval.

The stability and performance of the fixed gaits are investigated for varying walker parameters α, r, I_t, and k = 10, c = 10 (see Figure 7). The results indicate that stable walking is possible for I_t values of 0, 4, and 8. For $I_t = 0$, period-1 and period-2 gaits are observed for α values varied from 0.5 to 2. The transition from period-1 gaits to period-2 gaits is characterized by a maximum of the largest absolute eigenvalue (Figure 7a). The value of α at which the period-1 to period-2 transition occurs depends on other parameters; in the simulations, the transition seems to occur at around $\alpha = 1.5$. Below $\alpha = 0.5$ and above $\alpha = 1.8$, the largest eigenvalue modulus takes an almost constant value. For nonzero values of I_t, the period-1 to period-2 transition does not occur and the changes in maximum absolute eigenvalues with α and r are very similar (Figures 7b and 7c). The maximum absolute error of the torso depends on the selection of α and r (Figures 7d–7f). The higher the torso mass and its distance from the hip joint are, the higher the torso deviation error is. The highest of the torso error is still small, around 0.01 rad. The walking speed has a tendency to decrease with an increasing

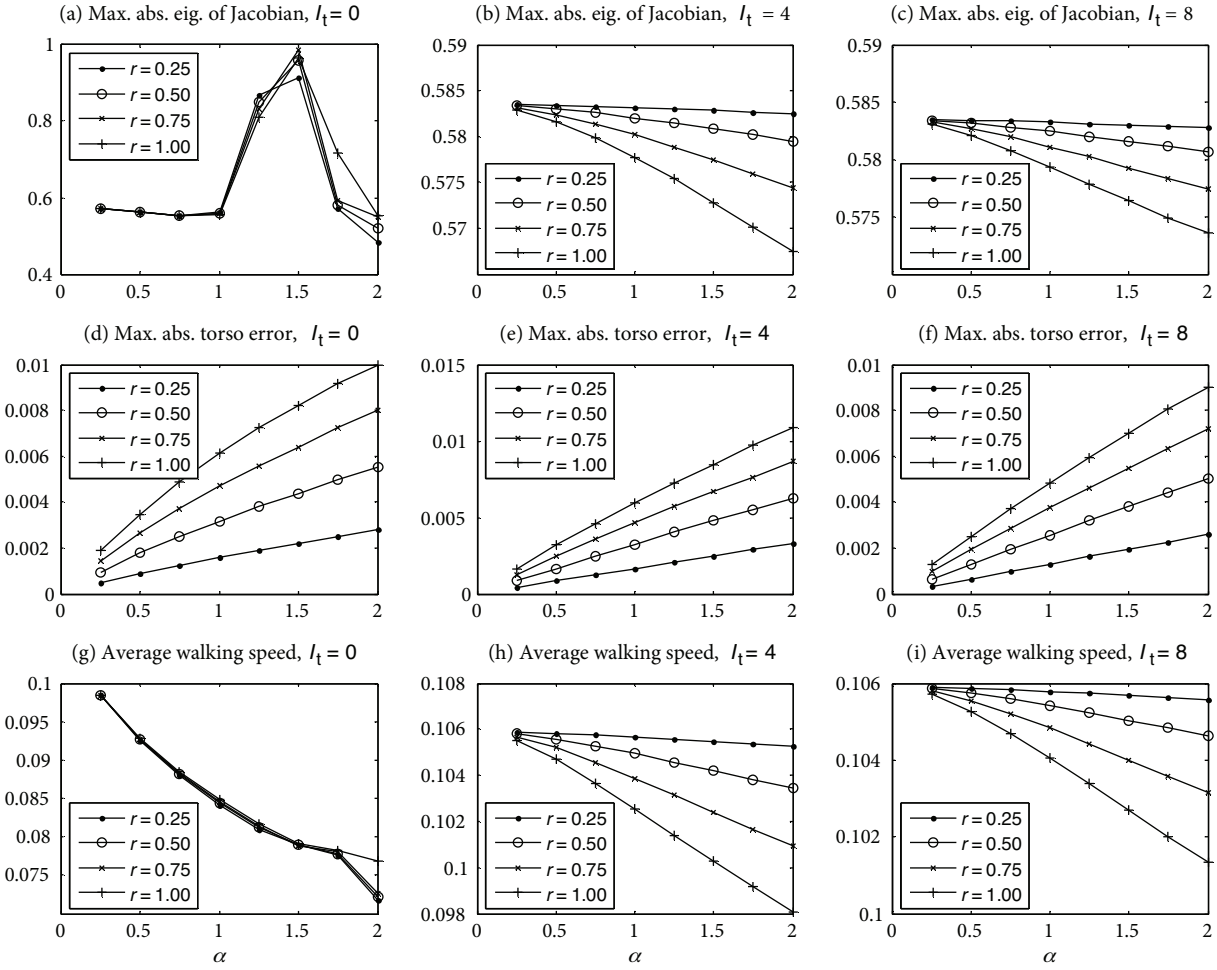

Figure 7. Stability and performance for the walker: $k = 10$, $c = 10$, and varying α, r, and I_t.

torso mass and its distance from the hip joint. For torso moment of an inertia greater than zero, the walking speed does not strongly depend on α and r (Figures 7g–7i).

6. Conclusions

It is shown that the compass-gait passive dynamic walker can be actuated to walk on level ground by a combination of hip/ankle torque and toe-off impulse. An equal hip/ankle torque applied to the active walker on small uphill slopes can mimic the trajectory for the passive walker on a downhill slope. Eigenvalue calculations indicate that the hybrid actuation method produces stable walking on level ground.

The addition of the torso mass and the PD control action result in stable walking with the torso kept in a vertical position. The computed torque method for the ankle joint reduces the dynamics of the walker to the fully passive walker. The amount of added mass to the hip joint has an effect on its stability, although it is possible to obtain stable walking for a torso mass of up to twice the hip mass. The walker with a torso exhibits mostly stable period-1 gaits. For the point torso mass ($I_t = 0$), certain values of the torso mass result in a transition from stable period-1 to period-2 gaits. The value of the torso mass, which gives transition from a period-1 gait to a period-2 gait, also yields a maximum of the largest absolute eigenvalue of the corresponding stride function.

In conclusion, the findings presented in this study can shed light on the design and development of walking-related mechanisms such as legged robots or walk assist devices. Analysis of passive walking devices such as the ones presented in this paper can also lead to a better understanding of the principles of natural walking.

References

[1] T. McGeer, "Passive dynamic walking", International Journal of Robotics Research, Vol. 9, pp. 68–82, 1990.

[2] T. McGeer, "Dynamics and control of bipedal locomotion", Journal of Theoretical Biology, Vol. 16, pp. 277–314, 1993.

[3] S.H. Collins, A. Ruina, "A bipedal walking robot with efficient and human-like gait", IEEE International Conference on Robotics and Automation, pp. 1983–1988, 2005.

[4] S. Collins, A. Ruina, R. Tedrake, M. Wisse, "Efficient bipedal robots based on passive-dynamic walkers", Science, Vol. 307, pp. 1082–1085, 2005.

[5] S.O. Anderson, M. Wisse, C.G. Atkeson, J.K. Hodgins, G.J. Zeglin, B. Moyer, "Powered bipeds based on passive dynamic principles", 5th IEEE/RAS International Conference on Humanoid Robots, pp. 110–116, 2005.

[6] M. Garcia, A. Chatterjee, A. Ruina, M. Coleman, "The simplest walking model: stability, complexity, and scaling", ASME Journal of Biomechanical Engineering, Vol. 120, pp. 281–288, 1998.

[7] M. Garcia, A. Chatterjee, A. Ruina, "Efficiency, speed, and scaling of 2D passive dynamic walking", Dynamics and Stability of Systems, Vol. 15, pp. 75–99, 2000.

[8] A. Kuo, "Energetics of actively powered locomotion using the simplest walking model", Journal of Biomechanical Engineering, Vol. 124, pp. 113–120, 2002.

[9] H. Ohta, M. Yamakita, K. Furuta, "From passive to active dynamic walking", International Journal of Robust and Nonlinear Control, Vol. 11, pp. 287–303, 2001.

[10] J.H. Choi, J.W. Grizzle, "Feedback control of an underactuated planar bipedal robot with impulsive foot action", Robotica, Vol. 23, pp. 567–580, 2005.

[11] F. Asano, M. Yamakita, K. Furuta, "Virtual passive dynamic walking and energy-based control laws", Proceedings of the IEEE/RSJ International Conference on Intelligent Robots and Systems, pp. 1149–1152, 2000.

[12] M. Coleman, A. Chatterjee, A. Ruina, "Motions of a rimless spoked wheel: a simple 3D system with impacts", Dynamics and Stability of Systems, Vol. 12, pp. 139–160, 1997.

[13] M. Wisse, A.L. Schwab, F.C.T. van der Helm, "Passive dynamic walking model with upper body", Robotica, Vol. 22, pp. 681–688, 2004.

[14] T. Chyou, G.F. Liddell, M.G. Paulin, "An upper-body can improve the stability and efficiency of passive dynamic walking", Journal of Theoretical Biology, Vol. 285, pp. 126–135, 2011.

[15] M. Gomes, A. Ruina, "Walking model with no energy cost", Physical Review E, Vol. 83, 2011.

[16] T. Narukawa, M. Takahashi, K. Yoshida, "Efficient walking with optimization for a planar biped walker with a torso by hip actuators and springs", Robotica, Vol. 29, pp. 641–648, 2011.

[17] R.W. Selles, J.B.J. Bussmann, R.C. Wagenaar, H.J. Stam, "Comparing predictive validity of four ballistic swing phase models of human walking", Journal of Biomechanics, Vol. 34, pp. 1171–1177, 2001.

[18] F.L. Buczek, K.M. Cooney, M.R. Walker, M.J. Rainbow, M.C. Concha, J.O. Sanders, "Performance of an inverted pendulum model directly applied to normal human gait", Clinical Biomechanics, Vol. 21, pp. 288–296, 2006.

[19] J.E. Boyd, "Synchronization of oscillations for machine perception of gaits", Computer Vision and Image Understanding, Vol. 96, pp. 35–59, 2004.

[20] M. Ekinci, "Human identification using gait", Turkish Journal of Electrical Engineering & Computer Sciences, Vol. 14, pp. 267–291, 2006.